



## Cosmic ray $^1\text{H}$ and $^2\text{H}$ spectra from BESS 98

Z.D. Myers<sup>a,\*</sup>, E.S. Seo<sup>a</sup>, J.Z. Wang<sup>a</sup>, R.W. Alford<sup>a</sup>, K. Abe<sup>b</sup>, K. Anraku<sup>b,1</sup>,  
 Y. Asaoka<sup>b</sup>, M. Fujikawa<sup>b</sup>, M. Imori<sup>b</sup>, T. Maeno<sup>d</sup>, Y. Makida<sup>c</sup>, H. Matsumoto<sup>b</sup>,  
 H. Matsunaga<sup>b,2</sup>, J. Mitchell<sup>e</sup>, T. Mitsui<sup>d,3</sup>, A. Moiseev<sup>e</sup>, M. Motoki<sup>b,3</sup>, J. Nishimura<sup>b</sup>,  
 M. Nozaki<sup>d</sup>, S. Orito<sup>b,4</sup>, J. Ormes<sup>e</sup>, T. Saeki<sup>b</sup>, T. Sanuki<sup>b</sup>, M. Sasaki<sup>e</sup>, Y. Shikaze<sup>d</sup>,  
 T. Sonoda<sup>b</sup>, R. Streitmatter<sup>e</sup>, J. Suzuki<sup>c</sup>, K. Tanaka<sup>c</sup>, I. Ueda<sup>b</sup>, N. Yajima<sup>f</sup>,  
 T. Yamagami<sup>f</sup>, A. Yamamoto<sup>c</sup>, T. Yoshida<sup>c</sup>, K. Yoshimura<sup>c</sup>

<sup>a</sup> *IPST, University of Maryland, College Park, MD 20742, USA*

<sup>b</sup> *Department of Physics, University of Tokyo, Bunkyo, Tokyo, 113-0033, Japan*

<sup>c</sup> *KEK, Tsukuba, Ibaraki, 305-0801, Japan*

<sup>d</sup> *Department of Physics, Kobe University, Kobe, Hyogo 657-8501, Japan*

<sup>e</sup> *NASA GSFC, Code 660, Greenbelt, MD 20771, USA*

<sup>f</sup> *ISAS, Sagami-hara, Kanagawa 229-8510, Japan*

Received 1 December 2002; received in revised form 9 October 2003; accepted 10 October 2003

### Abstract

The Balloon-borne Experiment with a Super-solenoidal Spectrometer (BESS) instrument has been flown annually from Lynn Lake Manitoba since 1993. The instrument has been upgraded several times to improve its performance. The instalment flown in 1998 was able to detect  $^2\text{H}$  clearly between 0.13 and 1.78 GeV/n as a result of improvements made on the time-of-flight (TOF) system. The BESS 98 data were analyzed to obtain the ratio and absolute fluxes of  $^1\text{H}$  and  $^2\text{H}$  over this energy range. The results were compared with different cosmic ray propagation models and their implications regarding their propagation history are discussed in this paper.

© 2004 COSPAR. Published by Elsevier Ltd. All rights reserved.

*Keywords:* Cosmic ray  $^1\text{H}$  and  $^2\text{H}$  spectra; BESS 98; Spallation; Secondary particles

### 1. Introduction

It is generally believed that  $^2\text{H}$  nuclei are secondary particles created from the spallation of primary cosmic rays, mainly H and He, during their Galactic propagation. The energy dependence of the ratio of the second-

aries to primaries can distinguish among Galactic propagation models. Accurate measurements of proton and deuterium spectra offer important knowledge regarding particle propagation in interstellar space. The Balloon-borne Experiment with a Super-solenoidal Spectrometer (BESS) was first launched in 1993. Since then these flights have been repeated annually, with each flight providing better results than the year before due to the continued improvements in the instrument's configuration. The 1998 flight was launched on July 29. During the 22 h flight, the instrument gathered 38 GB of data, which equated roughly to  $1.7 \times 10^7$  cosmic ray events. With its improved resolution, the 1998 instru-

\* Corresponding author. Tel.: +1-301-314-3239; fax: +1-301-314-9363.

<sup>1</sup> Currently at Kanagawa University.

<sup>2</sup> Currently at Tsukuba University.

<sup>3</sup> Currently at Tohoku University.

<sup>4</sup> Deceased.

ment could clearly distinguish protons from their  $^2\text{H}$  isotopes up to 1.78 GeV/n. This in turn provides extensive spectra for  $^1\text{H}$ ,  $^2\text{H}$ , and their ratio.

## 2. The BESS instrument

The BESS spectrometer was designed and constructed to conduct high-resolution searches for anti-matter in cosmic rays, and to make precise measurements of other cosmic ray components (Yamamoto et al., 1994; Ajima et al., 2000). A cross-section of the instrument's 98 configuration is shown below in Fig. 1.

All of the detector's components are assembled in a cylindrical configuration with a superconducting solenoidal magnet. The solenoid provides a uniform magnetic field of 1 T. The particle's trajectory is measured by a tracking system composed of several detectors in the instrument. Once the particle passes through the outer layer of the pressure vessel, it is detected by a time-of-flight (TOF) hodoscope on the upper part of the instrument. A similar hodoscope is located on the bottom of the instrument to detect the outgoing particles. These hodoscopes provide the velocity ( $\beta \equiv v/c$ ) and energy loss ( $dE/dx$ ) measurements. The data acquisition sequence is initiated by a first level TOF trigger, which is a coincidence of signals in the top and bottom scintillators. The TOF efficiency is estimated to be about 99.9% by examining the measured  $dE/dx$  distribution at the threshold level (Sanuki et al., 2000). The main parts of the tracking system consist of a central jet-type (JET) chamber and two inner drift chambers (IDC), which are used to determine a particle's rigidity. The Cerenkov

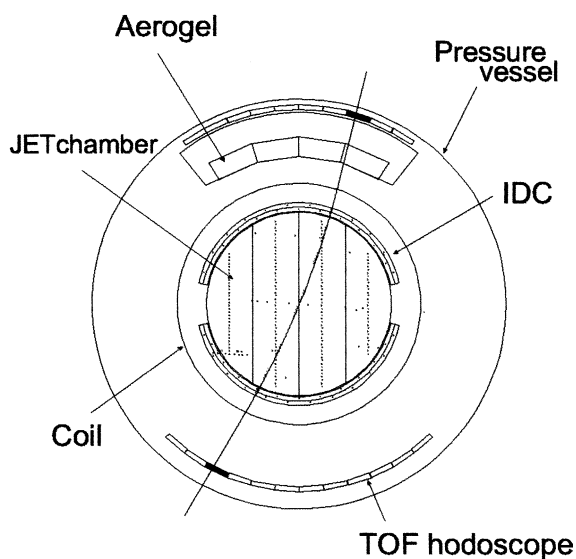


Fig. 1. Cross-section of the BESS instrument for the 98 flight. The curved line through the instrument depicts the track of an incoming particle.

counter with the aerogel radiator, which is able to detect events at high energies, was not used in the current isotope analysis. Improvements were also made to the TOF system from BESS 93 to BESS 98. By increasing the size of the photo-sensitive area of the hodoscopes, the number of photoelectrons was effectively increased. The time resolution, which is proportional to  $\sqrt{N_{\text{p.e.}}}$ , was improved from 300 to 75 ps. These improvements to the instrument were noticeable when analyzing the events with high energy.

## 3. Data analysis

### 3.1. Data selection

The BESS instrument was constructed to detect the fluxes of anti-matter. Since the number of events with negative rigidity is very small compared to events with positive rigidity, a biased trigger was used to limit the number of positive events recorded at low energies. However, for  $Z = 1$  and  $Z = 2$  particles, respectively, one event out of 60 and one event out of 25 were triggered without a bias. These events comprised the “countdown data set” used in this analysis. The particle ‘events’ that the BESS instrument detected were first separated by charge. The charge one ( $Z = 1$ ) and charge two ( $Z = 2$ ) candidates were selected by the charge cut, which was determined by the ionization energy loss ( $dE/dx$ ) of each event. Further cuts were applied to ensure single track events. Single track cuts selected events that had only one isolated track consisting of at least 16 hits through the central jet chamber and one or two hit counters in each layer of the TOF hodoscopes. The single-track selection eliminated events where nuclear interactions occurred inside the instrument. Further cuts were then applied to ensure track quality and consistency. With the data selection described above, 573,233 protons were identified in 1998. The overall efficiency of the cuts was then calculated to be 74%. Mass histograms were made for the remaining events to effectively separate  $^1\text{H}$  from  $^2\text{H}$ . Fig. 2 shows the mass histograms of  $^2\text{H}$  that fit well with Gaussian functions. Deuterium is clearly separated from the protons. The area of the Gaussian function was used as a particle count for  $^2\text{H}$ .

### 3.2. Absolute flux

In balloon experiments, secondary particles produced by nuclear interactions in the atmosphere are measured along with the primary cosmic ray events. Without correcting for these secondary particles the cosmic ray spectra at the top of the atmosphere cannot be correctly determined. The count spectra for  $^1\text{H}$  and  $^2\text{H}$  were corrected for atmospheric secondaries. Calculations for the

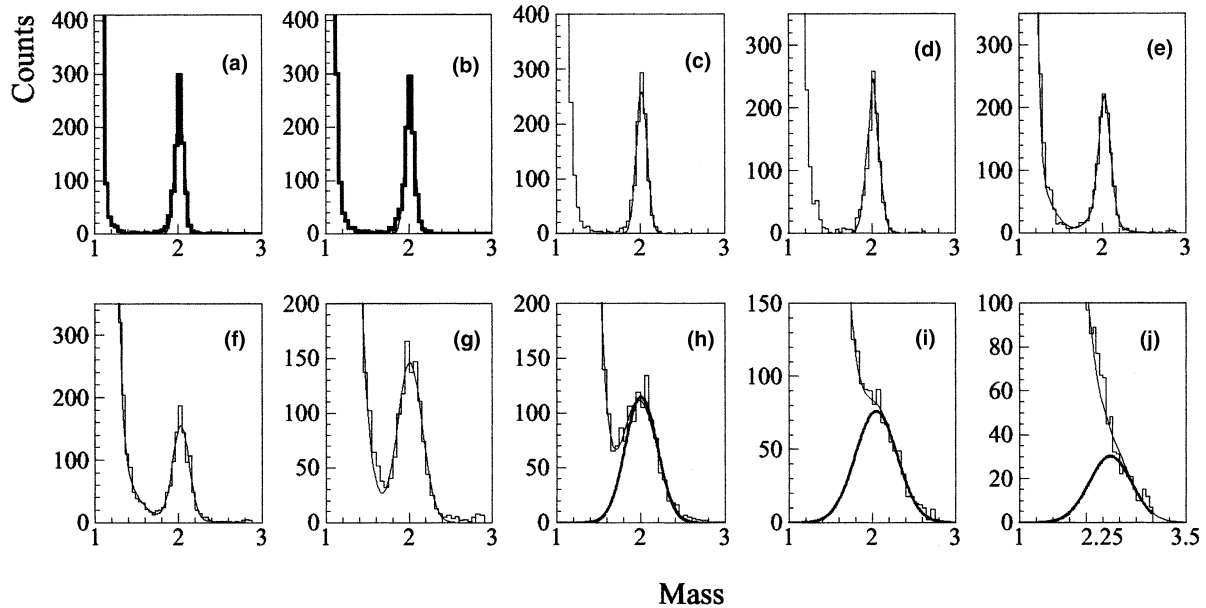


Fig. 2. Deuterium mass histograms for BESS 98 at the top of atmosphere detected over specific energy ranges. The energy ranges are in units of GeV/nucleon and are as follows: (a) 0.13–0.18; (b) 0.18–0.24; (c) 0.24–0.32; (d) 0.32–0.42; (e) 0.42–0.56; (f) 0.56–0.75; (g) 0.75–1.00; (h) 1.00–1.33; (i) 1.33–1.78; (j) 1.78–2.37.

atmospheric secondary deuterium were reported in Wang et al. (1999). The same method was used for the BESS 98 data analysis. The absolute flux was determined by the following:

$$F_{\text{TOA}}(E) = \left( \frac{N(E)C_d}{E_{\text{gr}}(E)E_c T \Delta E_{\text{in}}} - f_{\text{sec}}(E) \right) \frac{\Delta E_{\text{in}}}{\eta(E) \Delta E_{\text{TOA}}} \quad (1)$$

where  $C_d$  is the inverse of the countdown rate for  $Z = 1$  events (inverse of 1/60),  $E_{\text{gr}}$  is the effective geometry factor (calculated to be 0.21 m<sup>2</sup>sr),  $E_c$  is the efficiency of the data selection cuts,  $T$  is the live time (calculated to be 86.4% during the float time),  $\Delta E_{\text{in}}$  is the energy bin size

at the BESS float altitude and corresponds to  $\Delta E_{\text{TOA}}$  at the top of the atmosphere,  $f_{\text{sec}}(E)$  is the atmospheric secondary spectra, and  $\eta(E)$  is the correction factor for the attenuation loss (Wang et al., 2002).

#### 4. Results

The absolute fluxes of <sup>1</sup>H and <sup>2</sup>H obtained by analyzing the 98 data are shown in Figs. 3(a) and (b), respectively. The 1993 through 1998 spectra show annual variation that can be attributed to solar modulation.

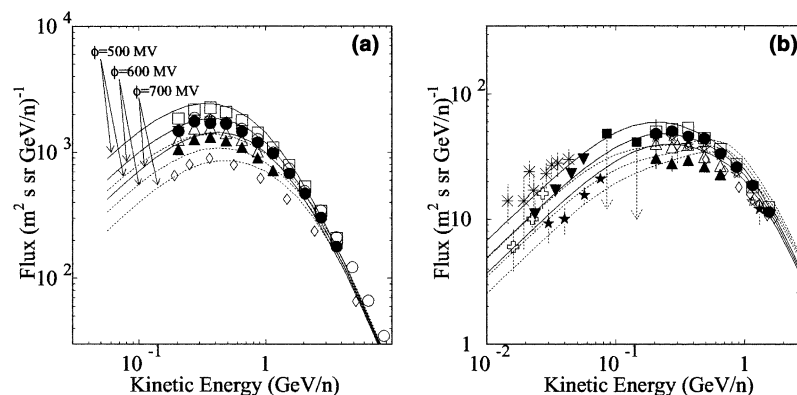


Fig. 3. Comparison of: (a) proton; (b) deuterium 98 fluxes with other data and with theoretical predictions of both a reacceleration model (solid curves) and the SLBM (dashed curves). Modulation parameters are 500, 600, 700 MV from top to bottom for both models. The data points are as follows: filled circles, BESS 98; open circles, Hydrogen from BESS 98; open squares, BESS 97, Wang et al. (1999); open stars, BESS 95, Wang et al. (1999); open upward pointing triangles, BESS 94, Wang et al. (1999); filled upward pointing triangles, BESS 93, Wang et al. (1999, 2002); open diamonds, de Nolfo et al. (2000), Menn et al. (2000); filled stars, Kroeger (1986), Bogomolov et al. (1995); filled squares, Leech and O’Gallagher (1978); filled downward pointing triangles, Beatty (1986); asterisks, Webber and Yushak (1983); open crosses, Mewaldt et al. (1976).

The solid curves represent calculated spectra using a reacceleration model with solar modulation parameters of 500 to 700 MV, reading from top to bottom. The dashed curves represent the calculated spectra using the standard leaky box model (SLBM) with the same modulation parameters. In the SLBM cosmic rays are trapped in the galaxy, which they fill uniformly, but have a certain probability of escaping into extragalactic space. Particles also lose energy from ionization energy loss during propagation through the interstellar medium. The escape length,  $X_e$ , is the mean thickness of matter traversed by cosmic rays. The escape lengths used here are the same as in Webber et al., 1992:  $X_e = 35.1\beta R^{-0.6} \text{ g cm}^{-2}$  for  $R \geq 3.3 \text{ GV}$  and  $X_e = 17.2\beta \text{ g cm}^{-2}$  for  $R \leq 3.3 \text{ GV}$ . In the Reacceleration model, stochastic reacceleration of the cosmic rays occurs from the turbulence, which supposedly exists in the interstellar medium. While this model requires the additional parameter  $\alpha$ , which determines the efficiency of reacceleration, the escape length is a simple power law in rigidity that reduces the number of total free parameters. The reacceleration model used in this analysis of cosmic ray transport involved two parameters which are the same ones used by Seo and Ptuskin (1994):  $14(R)^{-1/3} \text{ g cm}^{-2}$  for the power law escape length, and  $\alpha = 10^{-3} (\text{g cm}^{-2})^{-2}$  for the reacceleration efficiency. However, a smaller source abundance ratio,  $\text{H}/\text{He} \approx 11$ , was used in this analysis.

There is a noticeable difference in the shape of the  $^2\text{H}$  spectra calculated for the two models; the predicted spectra of the SLBM show a plateau between roughly 0.1 and 1 GeV/n while the predicted spectra of the reacceleration model peak at lower energies between 0.2 and 0.3 GeV/n. The BESS 98  $^2\text{H}$  spectrum, as well as earlier data, do not flatten out as the SLBM predicts. The location of the BESS 98 maximum flux is consistent with the reacceleration model.

The BESS 98  $^2\text{H}/^1\text{H}$  ratio shown in Fig. 4 is consistent with the BESS 93 ratio, within the range of uncertainty. The error bars represent only the statistical errors. The shaded regions show the overall systematic uncertainties. The uncertainties are higher at low energies, primarily because of secondary corrections. Theoretical models of the SLBM and the reacceleration are also compared with the data. The solid curves represent the reacceleration model and the dashed curves represent the SLBM. The three curves correspond to modulation parameters  $\phi = 700, 600, 500 \text{ MV}$ , reading from top to bottom. According to the SLBM, the data should increase from roughly 0.25 to 0.75 GeV/n and then decrease at higher energies. This bump structure predicted by the SLBM reflects the energy dependence of the  $^2\text{H}$  cross-sections. The BESS 98 ratio does not show any structure compatible with this peak predicted by the SLBM but, instead, shows a smooth decline that is consistent with

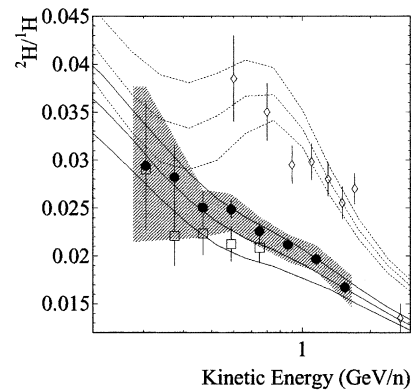


Fig. 4. The BESS ratio for  $^2\text{H}/^1\text{H}$  as compared with theoretical calculations. The data points are as follows: filled circles, BESS 98; open squares BESS 93, Wang et al. (2002); open diamonds IMAX 92 (de Nolfo et al., 2000), solid curves, reacceleration model (top to bottom, 700, 600, 500 MV); dashed curves, SLBM (top to bottom, 700, 600, 500 MV).

the reacceleration prediction. The IMAX 92 ratios (diamonds) are as high as the SLBM predicts but the data does not show any bump structure. The highest energy IMAX 92 data is more consistent with the reacceleration model.

The energy range where the bump occurs is also the range where the discrepancies between the predicted fluxes of the two models are the greatest. The difference in ratios due to different solar modulation levels is smaller than the difference due to the Galactic propagation effect.

## 5. Summary

The energy spectra for  $^2\text{H}$  and  $^1\text{H}$  as well as their ratios were measured with good precision over the energy range 0.18–1.78 GeV/n by analyzing the data from BESS 98. The BESS 98 flight was able to provide isotope measurements up to higher energies than previous BESS flights because of significant improvements in the instrument configuration. The  $^2\text{H}$  energy spectrum and the  $^2\text{H}/^1\text{H}$  ratio are both sensitive to propagation models. The BESS 98  $^2\text{H}$  spectrum shape agrees better with the reacceleration model. The  $^2\text{H}/^1\text{H}$  ratio does not show the structure expected from the SLBM and the ratio values are much lower than what the SLBM predicts above 0.4 GeV/n. It should be noted that the discrepancies between the predicted fluxes of the two models may, in part, be due to the method used in the theoretical calculations. They were calculated using a ‘weighted slab’ method, which does not provide an exact solution (Ptuskin et al., 1996). We are currently working to refine this method, in order to obtain exact solutions for the predicted spectra. We are also working on a similar analysis for  $^4\text{He}$  and its  $^3\text{He}$  isotope.

## Acknowledgements

This work has been supported in the USA by NASA grants NAG5-5347 and NAG5-5308, and in Japan by Grant-in-Aid for Scientific Research, MEXT and the Heiwa Nakajima Foundation. Further gratitude is extended to ISAS and KEK for their support of the BESS project.

## References

- Ajima, Y., Anraku, K., Haga, T. A superconducting solenoidal spectrometer for a Balloon-borne experiment. *Nucl. Instr. Methods A* 443, 71, 2000.
- Beatty, J.J. The isotopes of hydrogen and helium in the Galactic cosmic radiation — their source abundances and interstellar propagation. *Ap. J.* 311, 425–436, 1986.
- Bogomolov, E.A., Vasilyer, G.I., Krut'kov, Yu.S. The deuterium cosmic ray intensity from balloon measurement in energy range 0.8–1.8 GeV/n, in: *Proc. 24th ICRC*, vol. 2, pp. 598–601, 1995.
- de Nolfo, G.A., Barbier, L.M., Christian, E.R., et al. A Measurement of Cosmic Ray Deuterium from 0.5–2.9 GeV/nucleon. In: Medwaldt, R.A., et al. (Eds.), *Acceleration and Transport of Energetic Particles Observed in the Heliosphere*, AIP Conf. Proc., vol. 528. AIP, New York, p. 425, 2000.
- Kroeger, R. Measurements of hydrogen and helium isotopes in galactic cosmic rays from 1978 through 1984. *Astrophys. J.* 303, 816, 1986.
- Leech, H.W., O'Gallagher, J.J. The isotopic composition of cosmic-ray helium from 123 to 279 MeV/nucleon — a new measurement and analysis. *Astrophys. J.* 221, 1110–1123, 1978.
- Menn, W., Hof, M., Reimer, O., et al. The absolute flux of protons and helium at the top of the atmosphere using IMAX. *Astrophys. J.* 533, 281–297, 2000.
- Mewaldt, R.A., Stone, E.G., Vogt, R.E. The isotopic composition of hydrogen and helium in low-energy cosmic rays. *Astrophys. J.* 206, 616–631, 1976.
- Ptuskin, V.S., Jones, F.C., Ormes, J.F. On using the weighted slab approximation in studying the problem of cosmic-ray transport. *Astrophys. J.* 465, 972, 1996.
- Sanuki, T., Motoki, M., Matsumoto, H., et al. Precise measurement of cosmic-ray proton and helium spectra with the BESS spectrometer. *Astrophys. J.* 545, 1135–1142, 2000.
- Seo, E.S., Ptuskin, V.S. Stochastic reacceleration of cosmic rays in the interstellar medium. *Astrophys. J.* 431, 705–714, 1994.
- Wang, J.Z., Seo, E.S., Alford, R.W., et al. Isotopic Measurements of cosmic-ray hydrogen and helium during the 1997 solar minimum, in: *Proc. 26th ICRC*, vol. 3, pp. 37–40, 1999.
- Wang, J.Z., Seo, E.S., Anraku, K., et al. Measurement of cosmic-ray hydrogen and helium and their isotopic composition with the BESS experiment. *Astrophys. J.* 564, 244–259, 2002.
- Webber, W.R., Ferrando, P., Lukasiak, A., et al. Studies of the low-energy galactic cosmic-ray composition near 28 AU at sunspot minimum — the primary-to-primary ratios. *Astrophys. J.* 392, L91–L93, 1992.
- Webber, W.R., Yushak, S.M. A measurement of the energy spectra and relative abundance of the cosmic-ray H and He isotopes over a broad energy range. *Astrophys. J.* 275, 391–404, 1983.
- Yamamoto, A., Anraku, K., Golden, R., et al. Balloon-borne experiment with a superconducting solenoidal magnet spectrometer. *Adv. Space Res.* 14, 75–87, 1994.